ANTICANCER RESEARCH *37*: 475-480 (2017)
doi:10.21873/anticanres.11339

# Effect of Androgen on Normal Biodistribution of [$^{18}$F]-2'-Fluoro-5-methyl-1-beta-D-arabinofuranosyluracil ($^{18}$F-FMAU) in Athymic Non-tumor-bearing Male Mice

HOSSEIN JADVAR, RYAN PARK, LI-PENG YAP, KAI CHEN, LINDSEY HUGHES and PETER CONTI

*Department of Radiology, USC Molecular Imaging Center, Keck School of Medicine, University of Southern California, Los Angeles, CA, U.S.A.*

**Abstract.** *Aim: We assessed the association between the presence and absence of androgen on the normal biodistribution of the positron emission tomography (PET) cellular proliferation imaging biomarker, [$^{18}$F]-2'-Fluoro-5-methyl-1-beta-D-arabinofuranosyluracil ($^{18}$F-FMAU), in mice. Materials and Methods: Non-castrated (n=4) and castrated (n=4) athymic non-tumor-bearing male mice served as models for presence and absence, respectively, of androgen. MicroPET-CT scans were performed 1 h following tail vein administration of 200 uCi of $^{18}$F-FMAU. Imaging was performed at baseline and then at 7-day intervals longitudinally for 35 days only in castrated mice following subcutaneous introduction of a 12.5 mg, 21-day release, dihydrotestosterone pellet. Mean standardized uptake values ($SUV_{mean}$) were obtained for liver, heart, and muscle. Several two-group comparisons of average of $SUV_{mean}$ were performed. Results: Pre-pellet baseline average $SUV_{mean}$ (±s.d.) values in castrated mice were significantly lower than baseline non-castrated values, increased on day 15 and reached peak values on day 28, at which time they were significantly higher than corresponding baseline levels in both non-castrated and pre-pellet castrated mice. The peak values decreased significantly following dihydrotestosterone withdrawal. Conclusion: There is a significant modulatory effect of androgen on normal $^{18}$F-FMAU uptake levels in mice liver, heart and muscle tissues.*



*Correspondence to:* Hossein Jadvar, MD, PhD, MPH, MBA, USC Molecular Imaging Center, Department of Radiology, University of Southern California, 2250 Alcazar Street, CSC102, Los Angeles, CA 91107, U.S.A. Tel: +1 3234421107, Fax: +1 3234423253, e-mail: jadvar@med.usc.edu

*Key Words:* Androgen, prostate, FMAU, PET.

Positron emission tomography (PET) is destined to play an important role in the imaging evaluation of prostate cancer. This has been fueled by major strides in our fundamental understanding of the complex biology of this clinically heterogeneous disease and the design and synthesis of radiotracers that can track pathophysiological processes *in vivo*. The biological targets for imaging have included metabolites (*e.g.*, glucose, fatty acids, amino acids), antigens (*e.g.*, prostate-specific membrane antigen – PSMA), receptors (*e.g.*, androgen receptor, gastrin-releasing peptide receptor), angiogenesis, hypoxia, and gene-based pathways (1, 2). In few cases, theranostic companions have also been developed for targeted radionuclide therapy (*e.g.* $^{68}$Ga-PSMA for imaging and $^{177}$Lu-PSMA for therapy). Clinical research is actively being pursued to decipher the exact role of these agents along the natural history of prostate cancer.

We have previously reported on our initial pre-clinical observations on the potential usefulness of the cellular proliferation imaging biomarker, [$^{18}$F]-2'-fluoro-5-methyl-1-beta-D-arabinofuranosyluracil ($^{18}$F-FMAU), in characterizing prostate cancer (3). $^{18}$F-FMAU is a thymidine analogue that is phosphorylated by thymidine kinase, is incorporated into the DNA and tracks changes in mitochondrial thymidine kinase 2 (4). In our experiments that involved castrated and non-castrated mice, we made an interesting observation that $^{18}$F-FMAU uptake levels in organs may be influenced by androgen presence or absence.

The goal of the present study was to perform follow-up longitudinal imaging studies using non-tumor-bearing athymic mice before and after subcutaneous (*s.c.*) implantation of a time-release testosterone pellet to assess the effect of androgen on $^{18}$F-FMAU biodistribution in selected organs within same animals.

## Materials and Methods

*$^{18}$F-FMAU Radiosynthesis.* We have previously reported on a one-pot labeling procedure for the radiosynthesis of $^{18}$F-FMAU has

Table I. *Organ standardized uptake values at 1 h post-injection of $^{18}$F-FMAU.*

| $SUV_{mean}$ (avg.±s.d.) | Non-Castrated (n=4) | Castrated (n=4) | | | | | |
|---|---|---|---|---|---|---|---|
| Organ | | Pre-pellet | Day 7 | Day 15 | Day 21 | Day 28 | Day 35 |
| Liver | 1.12±0.04# | 0.83±0.07* | 0.76±0.14* | 0.97±0.15 | 1.27±0.12# | 1.55±0.17*# | 1.11±0.24 |
| Heart | 0.95±0.04# | 0.67±0.10* | 0.60±0.06* | 0.68±0.09* | 1.04±0.10# | 1.21±0.14*# | 0.77±0.18 |
| Muscle | 1.02±0.06# | 0.63±0.09* | 0.61±0.04* | 0.70±0.12* | 0.98±0.11# | 1.30±0.18*# | 0.79±0.18 |

*$p$<0.05 Compared to non-castrated; #$p$<0.05 compared to castrated (pre-pellet); s.d., standard deviation.

been described previously (5). $^{18}$F-FMAU is obtained at 12±3% radiochemical yield with 547mCi/umol specific activity, overall radiosynthesis time of about 150 minutes, and radiochemical purity of 99%.

*Animal preparation*. Non-castrated (n=4) and castrated (n=4) athymic male mice (Harlan Sprague Dawley, Indianapolis, IN) served as models for the presence and absence, respectively, of androgen. Our Institutional Animal Care and Use Committee and the Radiation Safety Committee approved all animal studies. Anesthesia was induced using 2% isoflurane in oxygen and maintained throughout all imaging studies. Euthanasia was performed by cervical dislocation while the animal was anesthetized. Animals were housed in the vivarium facility and were fed regular rodent food and water ad libidum. Dihydrotestosterone (DHT) pellets (Innovative Research of America, Sarasota, FL) were implanted *s.c.* only in the castrated mice using a trochar and the skin opening was closed with tissue glue Dermabond (Ethicon, Domerville, NJ). The pellet releases 12.5 mg of DHT payload over a period of 21 days nearly constantly with slight peak at day 1. The animals did not bear any tumors.

*MicroPET imaging*. MicroPET scans were performed on the microPET R4 (Concorde Microsystems, Knoxville, TN) and followed by microCT imaging (InveonCT, Siemens Medical Solutions USA, Knoxville, TN) for anatomic reference. Mice were anesthetized with inhalant anesthesia, 1-2% Isoflurane in oxygen, prior to intravenous administration of 200 uCi of $^{18}$F-FMAU and placed in their cage in an awakened state until scan time. Approximately 15 min prior to imaging, mice were induced with inhalant anesthesia and placed on the microPET scanner for imaging at 1 h post injection. Scans were reconstructed using Inveon Acquisition Workplace software (Siemens Medical Solutions, Malvern, PA, USA) and analyzed using Inveon Research Workspace (Siemens Medical Solutions, USA). PET data were all reconstructed using four iterations of the 2D-OSEM algorithm supplied by MicroPET Manager (Siemens Medical Solutions, USA) into 128 × 128×63 images with 0.084 mm × 0.084 mm × 1.21 mm spatial resolution. Computed tomographic (CT) images were acquired with the following setting: 80 kVp, 500 uA, 220 projections, 220 degress, 200 ms/projection, bin 4, 3072 pixels by 2048 pixels image, and 104 um voxel size. PET and CT images were co-registered using a phantom based transformation matrix. For each microPET-CT scan, regions of interest were drawn over the liver, left upper limb muscle, and the heart of the whole-body coronal images with multiple slices to create a 3D volume of interest mean concentration value. The mean value was converted to mean standardized uptake value using the following equation:

SUVmean=[3D mean concentration (uCi/cc)]/
[activity injected (uCi)/body mass (g)]

Imaging was first performed at baseline on 4 non-castrated and 4 castrated mice. The 4 castrated animals were then imaged longitudinally on days, 7, 15, 21, 28, and 35 following *s.c.* introduction of DHT pellet on day 0.

*Statistical data analysis*. Tissue tracer uptake level was calculated as mean standardized uptake value (SUVmean) from the PET data. Two-group comparisons of data were performed using a two-tailed Student *t*-test with unequal variance and significance probability level of less than 0.05.

## Results

Table I includes the average and standard deviations of the $SUV_{mean}$ at baseline in the 4 non-castrated mice and the 4 castrated mice at baseline and then at various time points after DHT pellet insertion. Figure 1 shows the average SUVmean of the liver, heart, and muscle tissues in non-castrated mice as well as castrated mice across each imaging time point before, during and after DHT pellet insertion.

The mean SUVs for 3 tissues were significantly different between non-castrated and castrated mice at baseline (liver: 1.12±0.04 *vs.* 0.83±0.07; heart: 0.95±0.04 *vs.* 0.67±0.10; muscle: 1.02±0.06 *vs.* 0.63±0.09, respectively, $p$<0.05). This difference remained in effect for all 3 organs on day 7 and for heart and muscle on day 15. The radiotracer uptake level in liver was consistently higher than those for the heart and muscle, with the latter two tissues demonstrating relatively similar uptake levels ($p$>0.05).

On day 15, average $SUV_{mean}$ increased and reached peak values on day 28 that was 7 days after end of DHT pellet hormonal release (liver: 1.55±0.17; heart: 1.21±0.14; muscle: 1.30±0.18) and were significantly different from corresponding tissue average $SUV_{mean}$ at their baseline levels in both castrate and non-castrate animals. The average SUVmean decreased significantly and relatively quickly

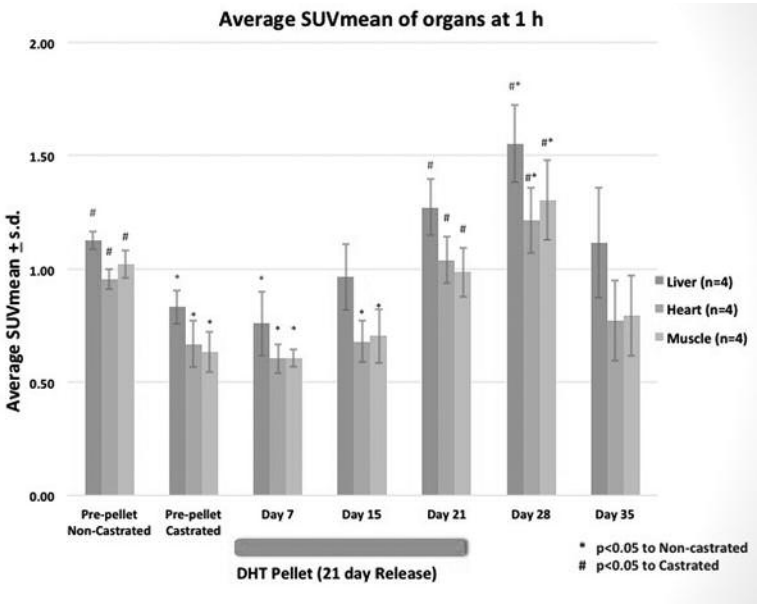


Figure 1. *Average $SUV_{mean}$ of liver, muscle and heart at 1 h post injection of $^{18}$F-FMAU in non-castrated and castrated athymic male mice at baseline and longitudinally in castrated mice following s.c. introduction of a 21-day release, 12.5 mg DHT pellet. Note the increase in tissue uptake of $^{18}$F-FMAU in relation to DHT release and subsequent decline in tissue uptake upon DHT withdrawal.*

from their peak level on day 28 to near baseline level on day 35 (14 days after the estimated end of DHT pellet hormonal release) and were not significantly different from either castrate or non-castrate baseline levels.

## Discussion

There have been major recent strides in the multimodal imaging assessment of prostate cancer at various phases along the natural history of the disease. These developments include multimodal imaging such as the recently commercialized PET/MR imaging system, increasing data on the potential utility of multiparametric MR imaging (*e.g.* diffusion weighted imaging, dynamic contrast enhanced imaging) and synthesis and testing of several novel promising PET radiotracers such as the recently FDA-approved synthetic L-leucine analogue, anti-1-amino-3-$^{18}$F-fluorocyclobutane-1-carboxylic acid (anti-$^{18}$F-FACBC, commercialized as Axumin™, Blue Earth Diagnostics, Oxford, UK), $^{18}$F- or $^{68}$Ga-PSMA, $^{68}$Ga-RM2 (targeted to gastrin releasing peptide receptor), and 16β-$^{18}$F-fluoro-5α-dihydrotestosterone ($^{18}$F-FDHT, targeted to the androgen receptor). Continued investigations with well-defined patient cohorts, independent validation, and comparative effectiveness studies will elucidate the utility of these PET radiotracers, either singly or as a combination, in the imaging evaluation of prostate cancer. Moreover, since some of these radiotracers are also amenable to pair with therapeutic counterparts (*e.g.* $^{68}$Ga-/$^{177}$Lu-PSMA), the role of theranostics is anticipated to grow (6).

Imaging assessment of cellular proliferation may allow for characterization of primary prostate cancer. Most prostate tumors are slow-growing. However, there are about 16% of inadvertently missed small-volume tumors at the time of biopsy that are clinically aggressive and may be amenable to focal therapy (7). Moreover, when castrate-sensitive state evolves into castrate-resistant state, the disease becomes more aggressive with a median survival of about 1-2 years (8).

PET in conjunction with radiotracers that track the thymidine salvage pathway of DNA synthesis has been studied relatively extensively for imaging of cellular proliferation in cancer (9). $^{11}$C-thymidine was initially evaluated but its use was limited due to rapid catabolism of thymidine and the short half-life (20 min) of $^{11}$C (10, 11). Further research resulted in the development of $^{18}$F-labeled analog with longer half-life (110 min) and resistance to catabolism. The most studied cellular proliferation PET radiotracer, 3'-deoxy-3'-fluorothymidine ($^{18}$F-FLT), is phosphorylated by cytosolic thymidine kinase 1 and retained in the proliferating cells without DNA incorporation (12, 13). Normal biodistribution of $^{18}$F-FLT shows relatively high uptake in the liver and the normal proliferating bone marrow (14). The physiologic high marrow accumulation of $^{18}$F-FLT severely limits its clinical utility in the assessment of bone metastases, which is common site of disease involvement in prostate cancer.

Another cellular proliferation agent, $^{18}$F-FMAU is also a thymidine analog that is phosphorylated preferentially by the mitochondrial thymidine kinase 2 and is incorporated in the DNA (4). Unlike $^{18}$F-FLT, $^{18}$F-FMAU shows little accumulation in bone that renders it potentially an ideal PET radiotracer for imaging cellular proliferation in prostate cancer (15). Limited observational studies of $^{18}$F-FMAU PET in prostate cancer have demonstrated retention of $^{18}$F-FMAU in local prostate recurrence, and in metastatic lesions with little activity in the urinary bladder and the normal bone (16, 17). We have also recently initiated a pilot study to assess the potential utility of $^{18}$F-FMAU in image-targeted biopsy using a software-based fusion of PET, transrectal ultrasound and multiparametric MR imaging of the prostate gland (18).

We hypothesized that $^{18}$F-FMAU PET may also be useful in characterizing primary tumor and predicting the transition from castrate-sensitive to castrate-resistant clinical state based on change in tumor cellular proliferation rate (19). Preclinical and clinical studies have shown that, although upon androgen deprivation in castrate sensitive tumor, there is a significant decline in tumor mass and cellular proliferation as measured by Ki67/MIB index, but then this is followed, after a period of time, by development of recurrent tumor growth and development of castrate-resistant state (20, 21). This phenotypic change may be multifactorial involving the androgen receptor-signaling axis (22). We set out to explore whether presence or absence of androgen affects the normal biodistribution of the cellular proliferation PET radiotracer $^{18}$F-FMAU in non-tumor bearing athymic male mice. We focused on 3 organ tissues of liver, muscle, and heart. Liver and muscle are often considered as internal background reference for target-to-background activity ratio calculations. Heart was also included in view of the organ's rich mitochondrial content, and given that the underlying biological basis for uptake of $^{18}$F-FMAU in the tissue is related to preferential phosphorylation by mitochondrial thymidine kinase 2. We showed that there is a statistically significant association between the presence or absence of androgen and the $^{18}$F-FMAU uptake levels in these 3 selected tissues. This suggests that there may be an association between androgen signaling and thymidine metabolism as depicted by $^{18}$F-FMAU PET. Exploration of the underlying biological mechanism for this observation was not in the scope of our imaging investigation. One possibility, however, may be the androgen control of mitochondrial function that can involve thymidine kinase 2 enzymatic activity (23). It is also interesting to note that observations in mice may potentially be different from those in humans. This is because there is a 10-fold lower competing circulating thymidine in humans than in mice (~0.15 μM *vs*. 1.5-3 μM, respectively) (24). The less competition for radiotracer uptake in humans may, therefore, potentially amplify the modulatory effect of androgens on $^{18}$F-FMAU biodistribution in human tissues but this supposition needs additional investigation in humans.

Our study was limited by not measuring the plasma level of testosterone at each imaging time point. However, the significant change in $^{18}$F-FMAU uptake levels in reference organs before, during and after androgen released by the pellet in castrated mice was supportive in that there was a modulatory association in this preclinical setting. We also did not measure the amount and activity levels of the relevant enzymes to corroborate with the imaging findings. Further studies measuring the content and bioactivity of both thymidine kinase 1 and thymidine kinase 2 in tissues will be needed. Nevertheless, there is a relatively strong suggestion that androgen modulates the tissue uptake level of the cellular proliferation imaging marker, $^{18}$F-FMAU, which may be an important consideration in the future preclinical animal and pilot human clinical studies.

## Conclusion

There is a significant association between androgen presence or absence and the level of $^{18}$F-FMAU uptake levels in normal liver, muscle and heart tissues as measured by microPET in non-tumor bearing athymic male mice. This suggests that assessment of $^{18}$F-FMAU PET studies in prostate cancer may need to take into account the effect of androgen-based treatments.

## Conflicts of Interest

None.

## Acknowledgements

Supported by the National Institutes of Health grants R21-CA142426, R21-EB017568, P30-CA01408 and the Whittier Foundation. The radiochemistry preparation and procedures for 18F-FMAU have been patented under US patent 7,273,600 B2 (inventors: P.S. Conti, M.M. Alauddin, J.D. Fissekis), and the patent has been assigned to the University of Southern California, Los Angeles, CA. None of the authors have any financial interest in this patent.

## References

1 Jadvar H: Molecular imaging of prostate cancer. Am J Roentgenology AJR *199*: 278-291, 2012.

2 Jadvar H: Positron emission tomography in prostate cancer: summary of systematic reviews and meta-analysis. Tomography *1*: 18-22, 2015.

3 Jadvar H, Yap LP, Park R, Li Z, Chen K, Hughes L, Kouhi A and Conti PS: [$^{18}$F]-2'-Fluoro-5-methyl-1-beta-D-arabinofurano-syluracil ($^{18}$F-FMAU) in prostate cancer: initial preclinical Observations. Mol Imaging *11*: 426-432, 2012.

4 Tehrani OS, Douglas KA, Lawhom-Crews JM and Shields AF: Tracking cellular stress with labeled FMAU reflects changes in mitochondrial TK2. Eur J Nucl Med Mol Imaging *35*: 1480-1488, 2008.

5 Li Z, Cai H and Conti PS: Automated synthesis of 2'-deoxy-2'-[$^{18}$F]fluoro-5-methyl-1-b-D-arabinofuranosyluracil ([$^{18}$F]-FMAU) using a one reactor radiosynthesis module. Nucl Med Biol *38*: 201-206, 2011.
6 Kulkarni HR, Singh A, Schuchardt C, Niepsch K, Sayeg M, Leshch Y, Wester HJ and Baum RP: PSMA-Based Radioligand Therapy for Metastatic Castration-Resistant Prostate Cancer: The Bad Berka Experience Since 2013. J Nucl Med *57*: 97S-104S, 2016.
7 Mazzucchelli R, Scarpelli M, Cheng L, Lopez-Beltran A, Galosi AB, Kirkali Z and Montironi R: Pathology of prostate cancer and focal therapy ('male lumpectomy'). Anticancer Res *29*: 5155-5161, 2009.
8 Pound CR, Partin AW, Eisenberger MA, Chan DW, Perason JD and Walsh PC: Natural history of progression after PSA elevation following radical prostatectomy. JAMA *281*: 1591-1597, 1999.
9 Bading JR and Shields A: Imaging of cell proliferation: status and prospects. J Nucl Med *49*: 64S-80S, 2008.
10 Conti PS, Alauddin MM, Fissekis JR, Schmali B and Watanabe KA: Synthesis of 2'-fluoro-5-[$^{11}$C]-methyl-1-beta-D-arabinofurasyluracil ([$^{11}$C]-FMAU): a potential nucleoside analog for *in vivo* study of cellular proliferation with PET. Nucl Med Biol *22*: 783-789, 1995.
11 Shields AF, Mankoff D, Graham MM, Zheng M, Kozaawa SM, Link JM and Krohn KA: Analysis of 2-carbon-11-thymidine blood metabolites in PET imaging. J Nucl Med *37*: 290-296, 1996.
12 Shields AF, Grierson JR, Dohmen BM, Machulla HJ, Stayanoff JC, Lawton-Crews JM, Obradovich JE, Muzik O and Mangner TJ: Imaging proliferation *in vivo* with [F-18]FLT and positron emission tomography. Nat Med *4*: 1334-1336, 1998.
13 Grierson JR and Shields AF: Radiosynthesis of 3'-deoxy- 3'-[18F]fluorothymidine: [$^{18}$F]FLT for imaging of cellular proliferation *in vivo*. Nucl Med Biol *27*: 143-156, 2000.
14 Vesselle H, Grierson J, Peterson LM, Muzi M, Mankoff DA and Krohn KA: $^{18}$F-fluorothymidine radiationdosimetry in human PET imaging studies. J Nucl Med *44*: 1482-1488, 2003.
15 Shields AF: Positron emission tomography measurement of tumor metabolism and growth: its expanding role in oncology. Mol Imaging Biol *8*: 141-150, 2006.
16 Sun H, Mangner TJ, Collins JM, Muzic O, Douglas K and Shields AF: Imaging DNA synthesis *in vivo* with $^{18}$F-FMAU and PET. J Nucl Med *46*: 292-296, 2005.
17 Sun H, Sloan A, Mangner TJ, Vaishampayan U, Muzik O, Collins JM, Douglas K and Shields AF: Imaging DNA synthesis with [$^{18}$F]FMAU and positron emission tomography in patients with cancer. Eur J Nucl Med Mol Imaging *32*: 15-22, 2005.
18 Jadvar H, Chen K and Ukimura O: Targeted Prostate Gland Biopsy With Combined Transrectal Ultrasound, mpMRI, and $^{18}$F-FMAU PET/CT. Clin Nucl Med *40*: e426-e428, 2015.
19 Jadvar H: Imaging cellular proliferation in prostate cancer with positron emission tomography. Asia Oceania J Nucl Med Mol Biol *3*: 72-76, 2015.
20 Agus DB, Cordon-Cardo C, Fox W, Dropnjak M, Koff A, Goldie DW and Scher HI: Prostate cancer cycle regulators: response to androgen withdrawal and development of androgen independence. J Natl Cancer Inst *91*: 1869-1876, 1999.
21 Kim D, Gregory CW, French FS, Smith GJ and Mohler JL: Androgen receptor expression and cellular proliferation during transition from androgen-dependent to recurrent growth after castration in CWR22 prostate cancer xenograft. Am J Path *160*: 219-226, 2002.
22 Scher HI and Sawyers CL: Biology of progressive, castration-resistant prostate cancer: directed therapies targeting the androgen-receptor signaling axis. J Clin Oncol *23*: 8253-8261, 2005.
23 Doeg KA, Polomski LL and Doeg LH: Androgen control of mitochondrial and nuclear DNA synthesis in male sex accessory tissue of castrate rats. Endocrinology *90*: 1633-1638, 1972.
24 Rustum YM: Fluoropyrimidines in cancer therapy. Totowa, NJ, Humana Press, Inc., p. 43, 2003.

*Received January 9, 2017*
*Revised January 19, 2017*
*Accepted January 20, 2017*